Locally Conservative Algorithms for Flow

Béatrice Rivière, Mary F. Wheeler and Eleanor Jenkins
Center for Subsurface Modeling
Texas Institute for Computational and Applied Mathematics
University of Texas, Austin, TX 78712

Abstract

Locally mass conservative methods for flow and transport are described and applications to the single phase flow and transport problems arising in porous media are presented. The pressure equation is solved either by a discontinuous Galerkin method or the mixed finite element method. The concentration equation is solved using a higher order Godunov method or by a discontinuous Galerkin method. Theoretical estimates are given in the case of the discontinuous Galerkin method. A velocity projection method based on the discontinuous Galerkin method is introduced. Numerical simulations comparing the methods are presented.

Introduction

In either surface water or subsurface water environmental quality modeling, the flow and multi-species transport may be solved separately using different numerical methods and grids due to differences in time and length scales involved. For example, in surface water, the flow grid usually needs to incorporate high resolution near land boundaries and should extend into the ocean to avoid spurious boundary effects. The transport code may only simulate transport over a small portion of the flow domain, and may use much coarser resolution. Therefore, for efficient coupling of flow and transport codes, it is critical to be able to take velocities from an arbitrary flow grid, and project them onto an arbitrary transport grid. For accurate multi-species transport, it is desirable for the velocities to be locally conservative on the transport grid.

Groundwater contaminant transport typically involves flow of one or more phases through a highly heterogeneous porous media, mass transfer between phases including the solid phases, advection with dispersion, and reaction of chemical and biological species. These phenomena, augmented by others such as heat transfer, and local injection and/or extraction of fluid, are closely coupled. On the discrete level, accuracy requires locally conservative schemes to maintain mass balances.

The computational complexity of both these applications demands a highly efficient approach. In general, it is not possible to solve the entire system of governing equations on the scale of the fastest reactions. Thus, out of necessity one must look at employing dynamic adaptive grids and using higher order methods.

For simplicity in this paper we restrict our attention to subsurface flows, although much of what is described can be applied to hydrodynamic flow problems where Chorin splitting or pressure stabilization techniques are used. We shall consider two schemes, mixed finite element methods and discontinuous Galerkin methods, which can be defined with arbitrary orders and are locally conservative.

This paper is divided into five additional sections. In Section , we describe the physical problem of single phase flow and transport in porous media. In Section , we formulate the discontinuous Galerkin method (DG) for solving the pressure and the concentration equations. Theoretical convergence results are summarized. In addition, a projection algorithm for obtaining a mass conservative velocity field is introduced. The latter provides a viable approach for the bay and estuary problem discussed above.

In Section , we briefly describe, the mixed finite element method (MFE) and the higher order Godunov method. Computational results for modeling flow and transport are presented for these methods in Section . In Section we conclude with some remarks and future research possibilities.

Subsurface Problem

The subsurface flow problem we are focusing on is the single phase flow and the transport of a contaminant in porous media. Numerical simulations of flow and transport play an important role in the engineering decisions about the exploitation of petroleum reservoirs and the control of groundwater pollution. We first state the governing equation for single phase flow, then the governing equation for transport in a domain $\Omega \subset I\!R^d, d = 1, 2, 3$:

$$-\nabla \cdot (K \nabla p) = q \quad \text{in} \quad \Omega, \tag{1}$$

$$p = p_0 \quad \text{on} \quad \Gamma_D, \tag{2}$$

$$K \nabla p \cdot \boldsymbol{\nu} = g \quad \text{on} \quad \Gamma_N, \tag{3}$$

where p denotes the pressure of the fluid, K is the permeability and measures the resistance of the medium to fluid flow. The boundary $\partial\Omega$ is the union of the Dirichlet (Γ_D) and Neumann (Γ_N) parts.

The transport of a contaminant in Ω over the time interval $J = (0, T]$ is described by

the following equations:

$$\begin{aligned}
\phi\frac{\partial c}{\partial t} + \nabla\cdot(\boldsymbol{u}c - D\nabla c) &= f \quad \text{in} \quad \Omega\times J, &(4)\\
(c\boldsymbol{u} - D\nabla c)\cdot\boldsymbol{\nu} &= c_{\text{in}}\boldsymbol{u} \quad \text{on} \quad \Gamma_{\text{in}}\times J, &(5)\\
-D\nabla c\cdot\boldsymbol{\nu} &= 0 \quad \text{on} \quad \Gamma_{\text{out}}\times J, &(6)\\
c(\cdot,0) &= c_0(\cdot) \quad \text{in} \quad \Omega, &(7)
\end{aligned}$$

where c denotes the concentration of the contaminant, $\boldsymbol{u}$ represents the Darcy velocity, the porosity ϕ is the fraction of the volume of the medium occupied by pores and D is the molecular diffusion and mechanical dispersion tensor. In general, D can be velocity dependent. The boundary conditions are mixed on the inflow part Γ_{in} and Neumann on the outflow part Γ_{out}. We recall that $\partial\Omega = \Gamma_{\text{in}}\cup\Gamma_{\text{out}}$ and that $\Gamma_{\text{in}} = \{x\in\partial\Omega : \boldsymbol{u}\cdot\boldsymbol{\nu} > 0\}$.

Discontinuous Finite Element Methods

Functional Settings

Let $\mathcal{E}_h = \{E_1, E_2, \ldots, E_{N_h}\}$ be a nondegenerate subdivision of Ω, where E_j is a triangle or a quadrilateral. The nondegeneracy requirement is that there exists $\rho > 0$ such that if $h_j = \text{diam}(E_j)$, then E_j contains a ball of radius ρh_j in its interior. Let $h = \max\{h_j, \quad j = 1\ldots N_h\}$. The edges of the polygon are denoted by $\{e_1,\ldots,e_{P_h},\ldots,e_{M_h}\}$ where $e_k\subset\Omega, 1\le k\le P_h$,and $e_k\subset\partial\Omega,\ P_h+1\le k\le M_h$. With each edge e_k , we associate a unit normal vector $\boldsymbol{\nu}_k$. For $k > P_h$, $\boldsymbol{\nu}_k$ is taken to be the unit outward vector normal to $\partial\Omega$.
For $s\ge 0$, let

$$H^s(\mathcal{E}_h) = \{v\in L^2(\Omega) : v|_{E_j}\in H^s(E_j), j = 1\ldots N_h\}.$$

We now define the average and the jump for $\phi\in H^s(\mathcal{E}_h),\ s > \frac{1}{2}$. Let $1\le k\le P_h$. For $e_k = \partial E_i\cap\partial E_j$ with $\boldsymbol{\nu}_k$ exterior to E_i for $i > j$ for some pair of elements (E_i, E_j), set

$$\{\phi\} = \frac{1}{2}(\phi|_{E_i})|_{e_k} + \frac{1}{2}(\phi|_{E_j})|_{e_k}, \quad [\phi] = (\phi|_{E_i})|_{e_k} - (\phi|_{E_j})|_{e_k}.$$

If the edge e_k belongs to the exterior boundary $\partial\Omega$, then we define

$$\{\phi\} = \phi, \quad [\phi] = \phi.$$

We denote the usual Sobolev norm by $\|p\|_{s,E}$ for $p\in H^s(E)$ and $E\subset I\!R^d$. We also define the following seminorm

$$|\!|\!|\phi|\!|\!|^2 = \sum_{j=1}^{N_h} \|K^{\frac{1}{2}}\nabla\phi\|^2_{0,E_j}$$

Let r be a positive integer. The finite element subspace is taken to be

$$\mathcal{D}_r(\mathcal{E}_h) = \{v : v|_{E_j} \in P_r(E_j) \quad \forall j\}$$

where $P_r(E_j)$ denotes the set of polynomials of (total) degree less than or equal to r on E_j, where E_j is a triangle or a quadrilateral.

Schemes

We describe a discontinuous Galerkin formulation of the problems (1)-(3) and (4)-(7). First, the pressure p is approximated by $P \in \mathcal{D}_r(\mathcal{E}_h)$ satisfying

$$\sum_{j=1}^{N_h} \int_{E_j} K\nabla P \cdot \nabla v - \sum_{k=1}^{M_h} \int_{e_k} \{K\nabla P \cdot \boldsymbol{\nu}_k\}\,[v] + \sum_{k=1}^{M_h} \int_{e_k} \{K\nabla v \cdot \boldsymbol{\nu}_k\}\,[P]$$
$$= \int_\Omega qv + \sum_{e_k \in \Gamma_D} \int_{e_k} (K\nabla v \cdot \boldsymbol{\nu}_k) p_0 + \sum_{e_k \in \Gamma_N} \int_{e_k} gv, \quad \forall v \in \mathcal{D}_r(\mathcal{E}_h).$$

The continuous-time approximation of the concentration of the contaminant is given by the map: $C : [0,T] \to \mathcal{D}_r(\mathcal{E}_h)$ determined by the relations

$$\int_\Omega \phi \frac{\partial C}{\partial t} w + \sum_{j=1}^{N_h} \int_{E_j} D\nabla C \nabla w - \sum_{j=1}^{N_h} \int_{E_j} C\boldsymbol{u} \cdot \nabla w + \sum_{k=1}^{P_h} \int_{e_k} C^* \boldsymbol{u} \cdot \boldsymbol{\nu}_k [w]$$
$$+ \sum_{e_k \in \Gamma_{\text{out}}} \int_{e_k} C\boldsymbol{u} \cdot \boldsymbol{\nu}_k w - \sum_{k=1}^{P_h} \int_{e_k} \{D\nabla C \cdot \boldsymbol{\nu}_k\}[w] + \sum_{k=1}^{P_h} \int_{e_k} \{D\nabla w \cdot \boldsymbol{\nu}_k\}[C]$$
$$= \int_\Omega qw - \sum_{e_k \in \Gamma_{\text{in}}} \int_{e_k} c_{\text{in}} \boldsymbol{u} \cdot \boldsymbol{\nu}_k w, \quad \forall w \in \mathcal{D}_r(\mathcal{E}_h),$$

where C^* is the upwind value of the concentration on a given edge. The discretization of the time derivative uses a backward-Euler method.

A Priori Error Estimates

The convergence of the discontinuous Galerkin method applied to single phase flow is proved in the following *hp* error estimates [9].

Theorem 1 *Let p be solution of (1)-(3). There is a constant M independent of h, r, p such that for $s \geq 2$*

$$|||p - P||| \leq M \frac{h^{\mu-1}}{r^{s-\frac{5}{2}}} ||p||_{s,\Omega},$$

where $\mu = \min(r+1, s)$.

The convergence of the discontinuous Galerkin method applied to linear transport is proved in the following *hp* error estimates [8]

Theorem 2 *Let c be solution of (4)-(7). If c belongs to $L^\infty(0,T;H^s(\Omega))$ and $\partial c/\partial t$ belongs to $L^2(0,T;H^s(\Omega))$, then there exists a constant M independent of h, r, c such that for $s \geq 2$*

$$\|c - C\|_{L^\infty(0,T;L^2(\Omega))} \leq M \frac{h^{\mu-1}}{r^{s-\frac{7}{2}}} \left(\|c\|_{L^\infty(0,T;H^s(\Omega))} + \|c\|_{L^\infty(0,T;H^s(\Omega))} \right),$$

where $\mu = \min(r+1, s)$.

DG Application: Locally Conservative Projection Algorithm for Changing Meshes

Let W_{h^o} and V_{h^n} be finite dimensional subspaces corresponding to the old and new meshes. Given $\boldsymbol{U}^{\mathrm{o}} \in W_{h^o}$, the problem is to find $\boldsymbol{U}^{\mathrm{n}} \in V_{h^n}$ such that the new velocity field is locally mass conservative. The new velocity can be expressed as

$$\boldsymbol{U}^{\mathrm{n}} = P_{h^n} \boldsymbol{U}^{\mathrm{o}} + \boldsymbol{\Gamma},$$

where P_{h^n} is a projection operator onto V_{h^n}. The local mass conservation implies

$$0 = \nabla \cdot \boldsymbol{U}^{\mathrm{n}} = \nabla \cdot P_{h^n} \boldsymbol{U}^{\mathrm{o}} + \nabla \cdot \boldsymbol{\Gamma}.$$

By writing $\boldsymbol{\Gamma} = \nabla \Phi$, the following elliptic problem is obtained

$$-\Delta \Phi = \nabla \cdot P_{h^n} \boldsymbol{U}^{\mathrm{o}}.$$

The elliptic problem is solved by using the discontinous Galerkin method: find Φ_h in $V_{h^n} \equiv \mathcal{D}_r(\mathcal{E}_h)$ such that

$$\sum_{j=1}^{N_h} \int_{E_j} \nabla \Phi_h \cdot \nabla \psi - \sum_{k=1}^{P_h} \int_{e_k} \{\nabla \Phi_h \cdot \boldsymbol{\nu}_k\} [\psi] + \sum_{k=1}^{P_h} \int_{e_k} \{\nabla \psi \cdot \boldsymbol{\nu}_k\} [\Phi_h] = \int_\Omega \nabla \cdot \boldsymbol{U}^{\mathrm{o}} \psi, \qquad \forall \psi \in \mathcal{D}_r(\mathcal{E}_h).$$

Mixed Finite Element and Godunov Methods

Let $W = L^2(\Omega)$ denote the set of square integrable functions and $H(\Omega; \mathrm{div}) = \{v \in (L^2(\Omega))^d \mid \nabla \cdot v \in L^2(\Omega)\}$. Let $V = \{v \in H(\Omega; \mathrm{div}) \mid v \cdot \nu = 0 \text{ on } \partial\Omega\}$. For

spatial discretization, we employ the lowest order Raviart-Thomas spaces $(W_h \times V_h)$ [7] defined over a rectangular grid of Ω with maximal grid spacing $h > 0$. $W_h \subset W$ consists of the space of piecewise constants and $\tilde{V}_h \subset H(\Omega; \mathrm{div})$ is the space of functions $v = (v_1, v_2, v_3)$ (if $d = 3$) such that v_i is continuous, piecewise linear over the grid in the ith direction and discontinuous, piecewise constant over the grid in the other two directions. We also need the subspace $V_h = \tilde{V}_h \cap V$.

We briefly describe the mixed finite element method for approximating (1). With $(\cdot, \cdot)$ denoting the $L^2(\Omega)$-inner product, we write (1) in variational form as

$$\begin{aligned} (K^{-1}\boldsymbol{u}, \boldsymbol{v}) - (p, \nabla \cdot \boldsymbol{v}) &= 0, \quad \boldsymbol{v} \in V, \\ (\nabla \cdot \boldsymbol{u}, w) &= (q, w), \quad w \in W. \end{aligned}$$

In the mixed finite element formulation, we seek the pair $(\boldsymbol{U}_h, P_h) \in V_h \times W_h$ satisfying

$$\begin{aligned} (K^{-1}\boldsymbol{U}_h, \boldsymbol{v}_h) - (P_h, \nabla \cdot \boldsymbol{v}_h) &= 0, \quad \boldsymbol{v}_h \in V_h, \\ (\nabla \cdot \boldsymbol{U}_h, w_h) &= (q, w_h), \quad w_h \in W_h. \end{aligned}$$

Chippada, Dawson, Martinez, and Wheeler formulated and analyzed a conservative projection method [1] based on a mixed hybrid finite element method for constructing mass conservation velocity fields. These results were for the lowest order mixed spaces; however, the analysis applies also to higher order approximating spaces.

An explicit, formally second order Godunov Godunov coupled with a mixed method is used for the concentration equation [3]. The scheme has a CFL time constraint but no spatial operator splitting is used, which helps reduce sensitivity to grid orientation. By introducing $z = -D\nabla c$, and defining $q^n = q(\cdot, t^n), c^n = c(\cdot, t^n)$, we solve for $(C^n, Q^n) \in V_h \times W_h$ such that

$$\begin{aligned} (D^{-1}Q^n, \boldsymbol{v}) - (C^n, \nabla \cdot \boldsymbol{v}) &= -(c_{\mathrm{in}}, \boldsymbol{v} \cdot \boldsymbol{\nu}), \quad \forall \boldsymbol{v} \in V_h, \\ (\frac{C^n - C^{n-1}}{\Delta t^n}, w) + (\nabla \cdot Q^n, w) &= -(\nabla \cdot G^{n-1}, w), \quad \forall w \in W_h, \end{aligned}$$

where G^n is the numerical flux obtained by using a Godunov method.

Numerical Results

Single Phase Flow in a Layered Porous Media

Our first example consists of a layered porous media with highly varying permeabilities. This example is a benchmark problem designed by the engineers of ANDRA [2].

We will compare the pressure fields obtained by the discontinuous Galerkin and the mixed finite element methods. The two-dimensional domain $(0, 25000) \times (0, 695)$ is shown on Fig. 1 and the permeabilities are given in the following table. The boundary conditions are the following

$$\begin{aligned} p &= 289 \quad \text{on} \quad \{25000\} \times \{0, 200\}, \\ p &= 310 \quad \text{on} \quad \{25000\} \times \{350, 595\}, \\ p &= 180 + 160x/25000 \quad \text{on} \quad \{0, 25000\} \times \{695\}, \\ p &= 200 \quad \text{on} \quad \{0\} \times \{295, 595\}, \\ p &= 286 \quad \text{on} \quad \{0\} \times \{0, 200\}, \\ K\nabla p \cdot \boldsymbol{\nu} &= 0 \quad \text{elsewhere.} \end{aligned}$$

The computational meshes for DG and MFE are shown in Fig. 2. The pressure fields are shown in Fig. 3. We note that the DG approximation is solved on a coarser mesh than the MFE approximation. The number of degrees of freedom is 3024 for DG and 8800 for MFE. The isocontours obtained with both methods are almost identical.

Single Phase Flow in a Fractured Rock

We compared the flow patterns in a fractured rock using both the mixed finite element method and the discontinuous Galerkin method. In this test case, two inclined fracture zones intersect one another at depth. The medium is isotropic but the value of the permeability is higher in the fracture zones ($K = 10^{-6} ms^{-1}$) than in the surrounding rock ($K = 10^{-8} ms^{-1}$). The boundary of the region is assumed to be impermeable to flow except for the top boundary (Γ_D) (see Fig. 4), where we impose the following condition:

$$p(x, y) = y, \quad \forall (x, y) \in \Gamma_D.$$

A more detailed description can be found in [4]. Fig. 5 shows the pressure field. The discontinuous Galerkin method is applied with a cubic order of approximation. The lowest order Raviart-Thomas space is used for the mixed method. Fig. 6 shows the velocity field obtained with both methods. The results are very similar and show that the flow is concentrated in the fracture zones as expected.

Locally Conservative Projections: RIPRAP Facility

Locally conservative flow fields are needed for water quality tranport codes, such as CE-QUAL-ICM, to ensure that mass balances are accurate. For applications at the U.S. Army Corps of Engineers Engineer Research and Development Center (ERDC), the hydrodynamic flow fields are generated by TABS-MDS, which is an adaptation

of the RMA-10 code [5] and which in general does not provide locally conservative flows. Therefore, we use mixed methods in the projection algorithm UTProj3D to construct flow fields with this property.

UTProj3D solves for the mass correction of a 3D velocity field as the solution to an elliptic boundary value problem with appropriate boundary conditions on the hydrodynamic mesh. The UTProj3D discretization is based upon the hybrid mixed-finite element method using tetrahedral, hexahedral, and prismatic elements. This discretization of the elliptic problem is known to conserve mass element-by-element [1]. A zero flux boundary condition is chosen for the water surface velocity correction and for the inflow boundaries. The latter ensures that no modification is made to the inflow rate. Flux boundary conditions cannot be used everywhere, as this defines a pure Neumann problem which produces a singular matrix having a one-dimensional null space. This problem is removed by using zero pressure boundary conditions for the correction velocity at the outflow boundary.

The following figures show the results from a test problem provided by Charlie Berger and Gary Brown of ERDC. The test mesh is a model of the riprap facility located at the ERDC in Vicksburg, MS. Fig. 7 shows a plan view of the test mesh, and Fig 8 shows the mass errors before and after the projection algorithm is applied.

Linear Transport

This benchmark problem [6] consists of simulating the propagation of a tracer in a 45 degrees flow pattern. Parameters used in the calculation are: a fluid flow velocity of $15.768my^{-1}$ along the positive x and y axes, diffusion coefficient equal to $10^{-5}cm^2s^{-1}$ and porosity equal to 1. The computational grid on the domain $(0, 10)^2$ is structured and consists of 50×50 cells. This gives a grid Peclet number of 100. The initial concentration consists of a concentration mound of unit concentration with a width of $2m$ occupying the square region $(1, 3)^2$. The concentration is zero elsewhere. Zero gradient boundary conditions are imposed around the periphery of the domain. A Courant number of 0.1 is used in the calculation and the simulation is run for $5.10^6 s$. The contours obtained with the discontinuous Galerkin and the higher order Godunov methods are shown in Fig. 9. We observe that there is less numerical diffusion in the case of the DG approximation.

Conclusions

A new higher order locally conservative scheme for computing Darcy flow has been presented. Computational results indicate that concentration grids can be coarser for higher order velocity approximations. Our current research is to investigate the use of different grids for concentration and for flow.

Acknowledgments

This work was funded by the DoD High Performance Computing Modernization Program U.S. Army Engineer Research and Development Center (ERDC) Major Shared Resource Center through Programming Environment and Training (PET), supported by Contract Number: DAHC 94-96-C0002, Computer Sciences Corporation.

The authors would like to thank Charlie Berger and Gary Brown of the ERDC with their help in generating the UTProj3D test problem, and Victor Parr for his work in running the test problem. The authors would also like to thank Krzysztof Banas, Steve Bryant and Xiuli Gai for their help in running some of the test cases.

References

[1] S. Chippada, C.N. Dawson, M.L. Martinez and M.F. Wheeler (1998). A projection method for constructing a mass conservative velocity field. In *Computer Methods in Applied Mechanics and Engineering: Proceedings of the 1997 Symposium on Advances in Computational Mechanics*, volume 157, pages 1–10.

[2] ANDRA Couplex test cases (February 2001). Results presented to scientific committee, Paris.

[3] C.N. Dawson (1993). Godunov-mixed methods for advection-diffusion equations in multidimensions. *SIAM J.Numer.Anal.*, 30(5):11315–1332.

[4] E.F. Kaasschieter (1995). Mixed finite elements for accurate particle tracking in saturated groundwater flow. *Advances in Water Resources*, 18(5):277–294.

[5] I.P. King (1993). RMA-10, a finite element model for three-dimensional density stratified flow. Technical report, Department of Civil and Environmental Engineering, University of California, Davis.

[6] P.C. Lichtner (1997). Benchmark problem: transporting a conservative tracer in a flow pattern 45 degrees to a rectangular cartesian 2d grid. http://terrassa.pnl.gov:2080/ kash/workshop/.

[7] P.A. Raviart and J.M. Thomas (1977). A mixed finite element method for second order elliptic problems. *Mathematical Aspects of the Finite Element Method, Lecture Notes in Mathematics*, 606:292–315.

[8] B. Rivière and M.F. Wheeler. Error analysis of discontinuous finite element methods for transport with nonlinear reaction. In preparation.

[9] B. Rivière, M.F. Wheeler and V. Girault (2000). A priori error estimates for finite element methods based on discontinuous approximation spaces for elliptic problems. *SIAM J. Numer. Anal.* To appear.

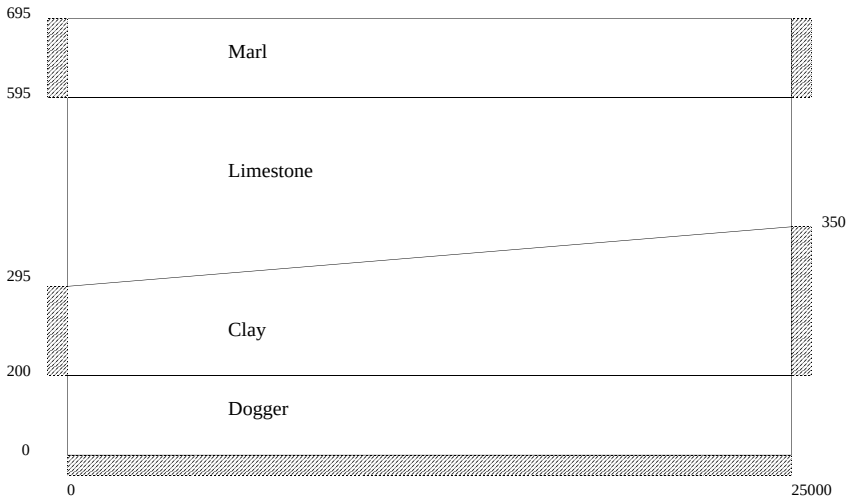

Figure 1: Geometry of computational domain

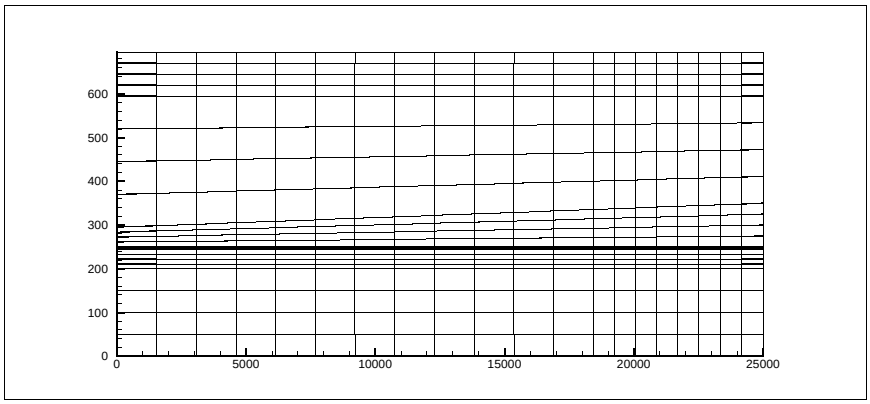

(a)

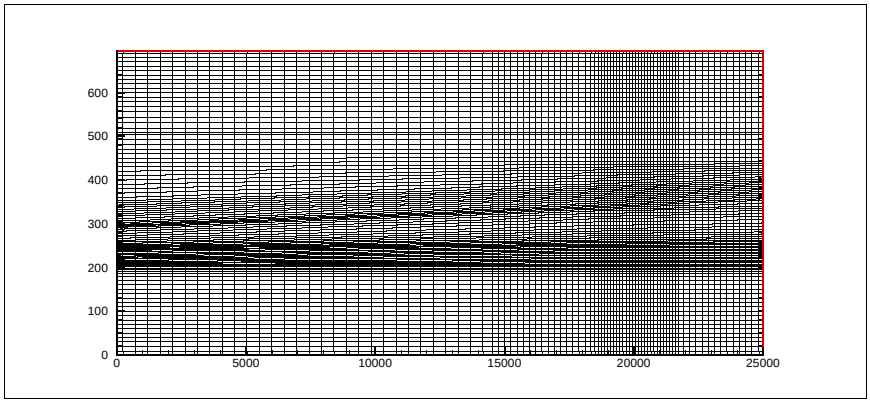

(b)

Figure 2: Meshes (a) DG (20x24) (b) MFE (88x100).

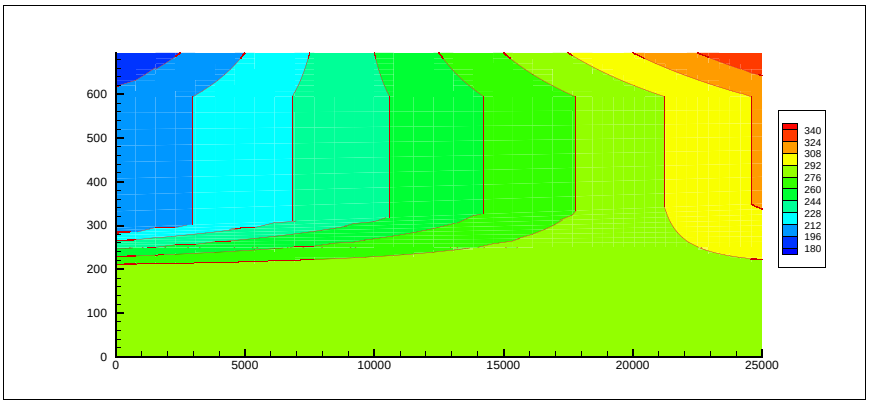

(a)

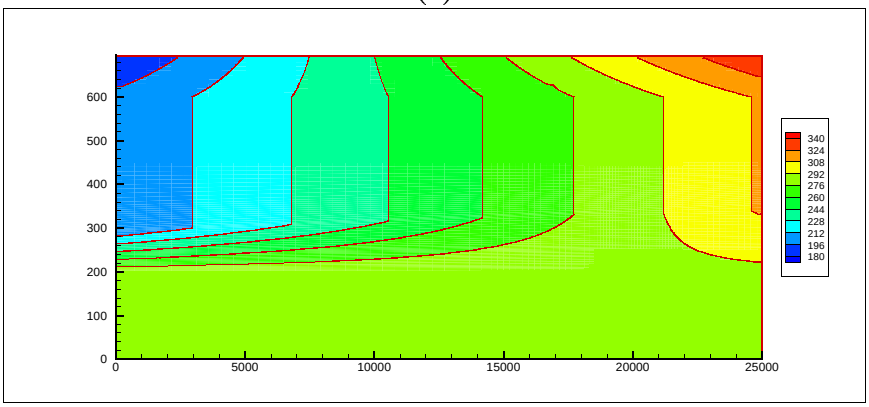

(b)

Figure 3: Pressure field: (a) DG 3024 dofs and (b) MFE 8800dofs.

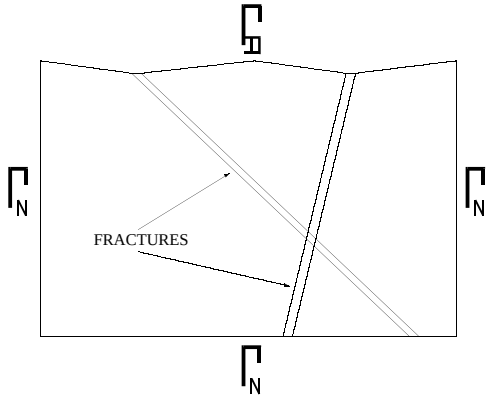

Figure 4: Diagram of the problem showing the fracture zones and the boundary conditions

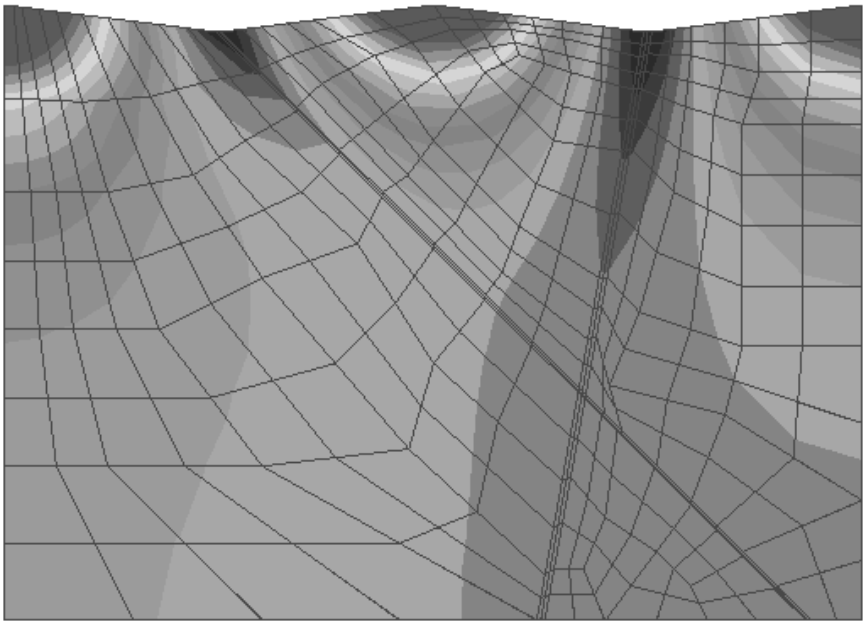

(a)

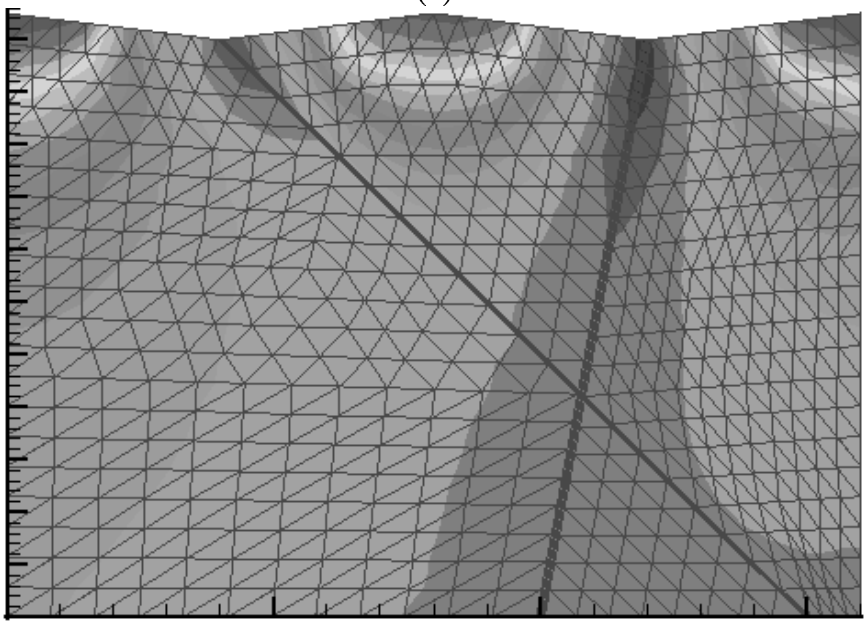

(b)

Figure 5: Pressure Field: (a) DG cubic approximation and (b) MFE

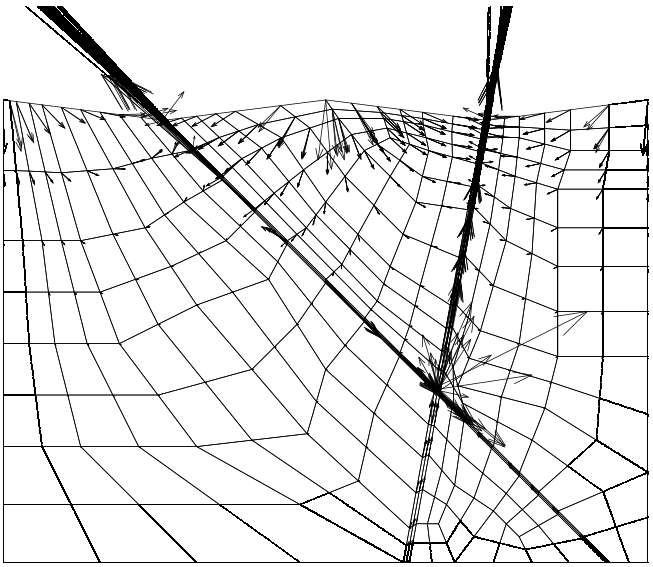

(a)

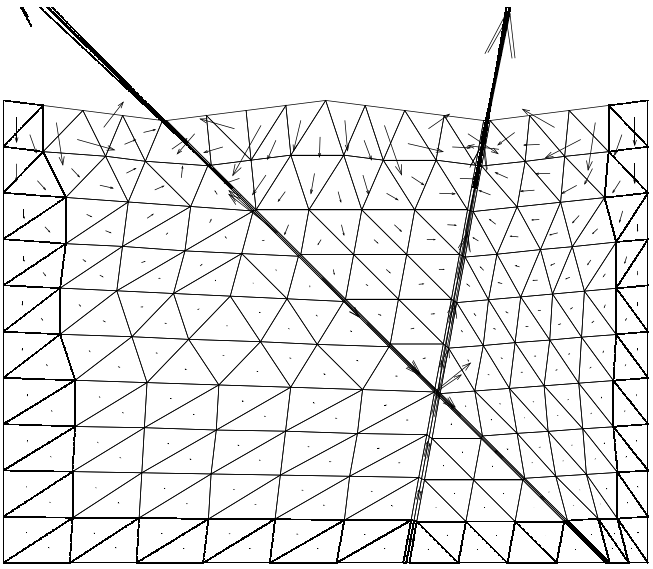

(b)

Figure 6: Velocity Field: (a) DG $r = 3$ and (b) MFE

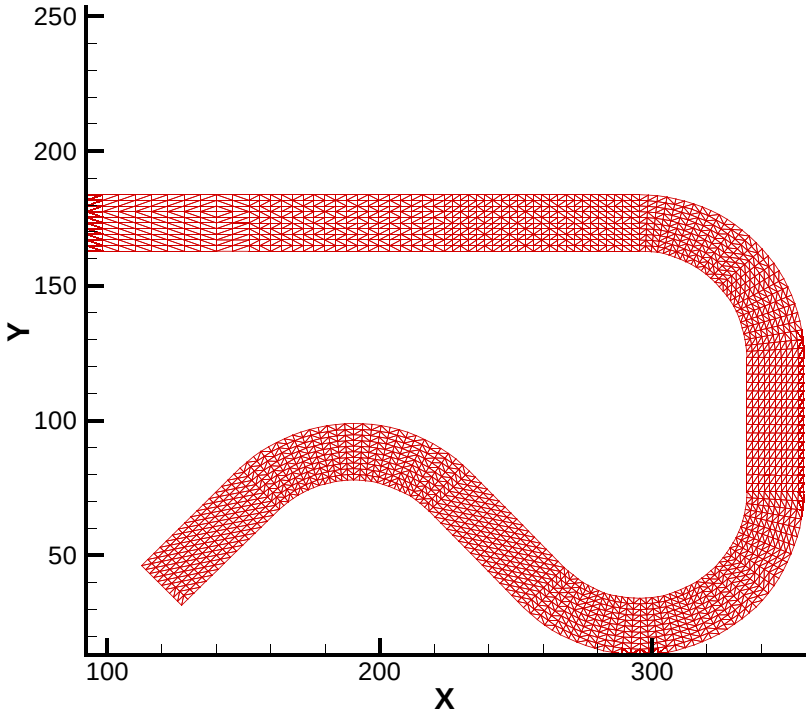

Figure 7: Plan view of test mesh

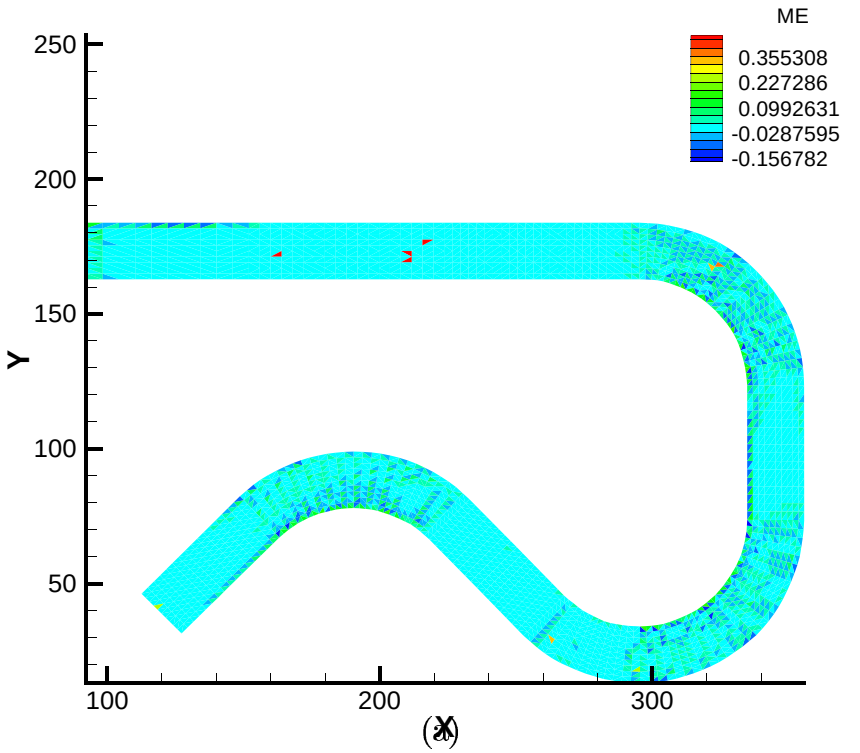

(a)

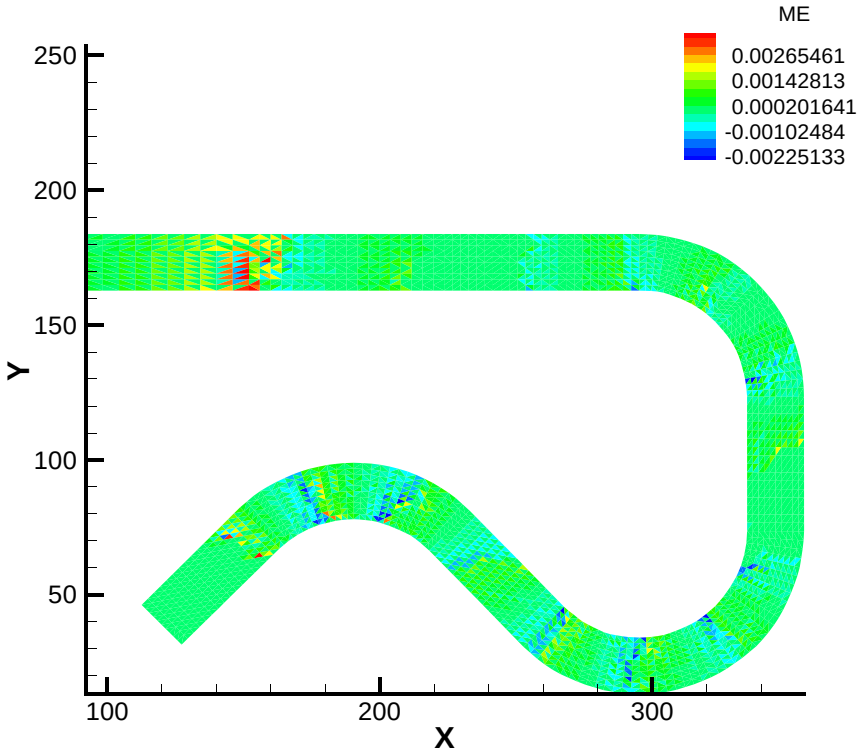

(b)

Figure 8: Local mass errors (a) before mass-error reduction (b) after mass error reduction

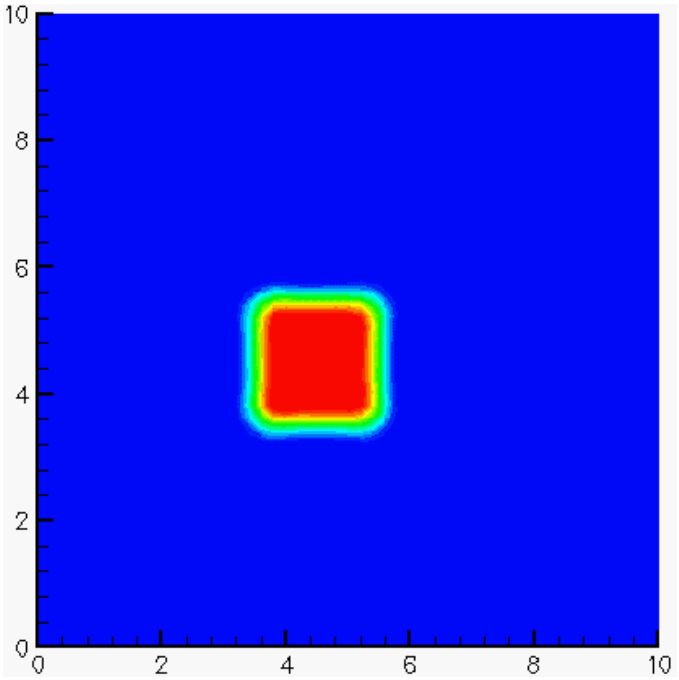

(a)

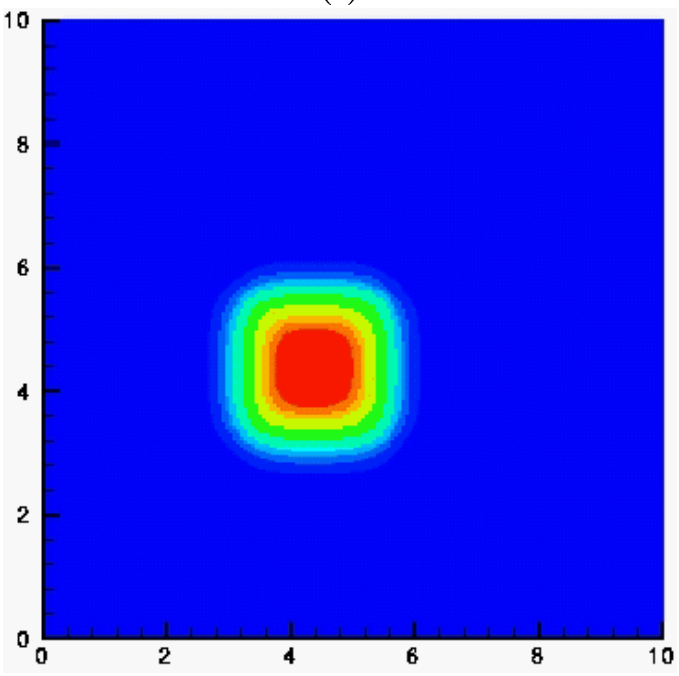

(b)

Figure 9: Concentration contour: (a) discontinuous Galerkin (b) higher order Godunov

	Marl	Limestone	Clay	Dogger
K(m/year)	3.1536e-5	6.3072	3.1536e-6	25.2288

Table 1: Permeability tensor in the four rock layers